nature portfolio

https://doi.org/10.1038/s41586-022-04747-5

Supplementary information

Mitochondrial uncouplers induce proton leak by activating AAC and UCP1

In the format provided by the authors and unedited

Mitochondrial Uncouplers Induce Proton Leak by Activating AAC and UCP1

Ambre M. Bertholet[1,2♣], Andrew M. Natale[3♣], Paola Bisignano[3], Junji Suzuki[1], Andriy Fedorenko[1], James Hamilton[4], Tatiana Brustovetsky[4], Lawrence Kazak[5], Ryan Garrity[5], Edward T. Chouchani[5], Nickolay Brustovetsky[4], Michael Grabe[3*], and Yuriy Kirichok[1*]

[1]Department of Physiology, University of California San Francisco, San Francisco, CA, USA.

[2]Department of Physiology, David Geffen School of Medicine, University of California Los Angeles, Los Angeles, CA, USA.

[3]Cardiovascular Research Institute, Department of Pharmaceutical Chemistry, University of California San Francisco, San Francisco, CA, USA.

[4]Department of Pharmacology and Toxicology, School of Medicine, Indiana University, Indianapolis, IN, USA.

[5]Dana-Farber Cancer Institute & Department of Cell Biology, Harvard Medical School, Boston, MA, USA.

*Correspondence to: Michael.Grabe@ucsf.edu (M.G.) and Yuriy.Kirichok@ucsf.edu (Y.K.).

♣These authors contributed equally to this work.

Content

Supplementary Figure 1. Gel source data

Extended Data Figure 3g

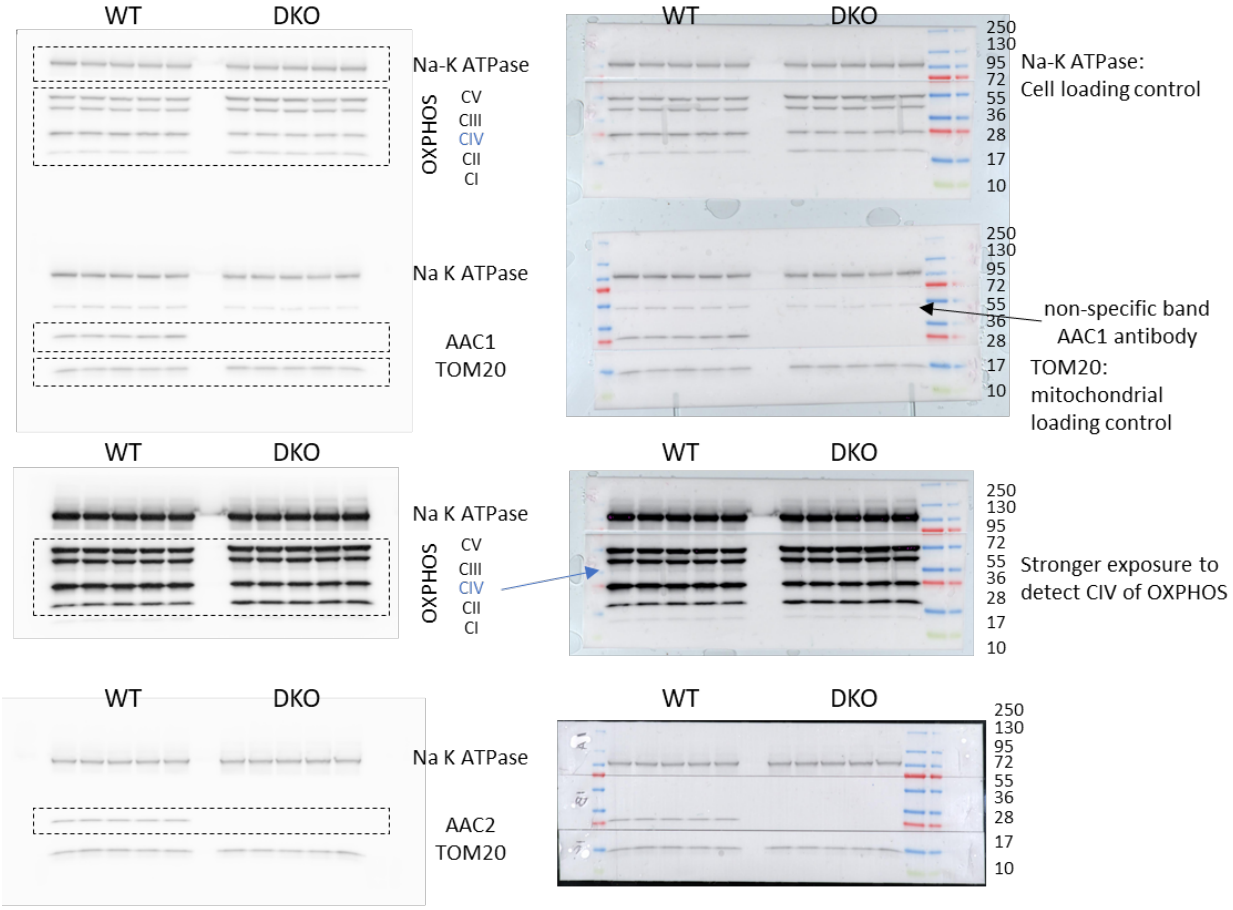

Lines 1 to 5 : WT C2C12 cell lines
Lines 6 to 10 : DKO AAC1/AAC2 C2C12 cell lines

Rectangles indicate the part of the image cropped for Extended Data Fig. 3g.

Supplementary Text 1. Mathematical model of uncoupler-aided H^+ permeation through AAC.

1 A three-state proton pathway model of proton uncoupling.

Assume that the uncoupler is at saturating concentrations such that it is bound to the transporter with unitary probability. Next, we assume that the transporter has already undergone a transition to open a proton pathway, which may be a slow transition requiring milliseconds, from the central cavity to the matrix, but we do not make any assumptions about the nature of this pathway (i.e. structured water wire, larger disordered aqueous pathway, protonatable site on protein, etc.) other than it can be described by Arrhenius-like rate constants. These three distinct states are pictured in Fig. 4g of the main text, and the corresponding differential equations describing the evolution of these states are:

$$\frac{dx_1}{dt} = -(k_c^{on} + k_m^{on})x_1 + k_c^{off}x_2 + k_m^{off}x_3 \quad (1)$$

$$\frac{dx_2}{dt} = -\left(k_c^{off} + k_{23}\right)x_2 + k_c^{on}x_1 + k_{32}x_3 \quad (2)$$

$$\frac{dx_3}{dt} = -\left(k_m^{off} + k_{32}\right)x_3 + k_{23}x_2 + k_m^{on}x_1 \quad (3)$$

where $\mathbf{x_1}$ is the AAC1-uncoupler system with no proton bound, $\mathbf{x_2}$ is the system with a proton bound to the uncoupler, $\mathbf{x_3}$ is the system with a proton in the matrix pathway, and there are several rate constants k that describe the rates for moving between these states. The first primary proton binding/unbinding step is binding to the AAC1-uncoupler complex in state x_1 from the cytoplasm/IMS (k_c^{on}) and then reversible unbinding (k_c^{off}) from state x_2. The second binding/unbinding transitions occur as the proton unbinds to the matrix from the matrix pathway (k_m^{off}) x_3 back to x_1 or binds to the matrix pathway from the lumen of the mitochondria (k_m^{on}). The rate k_{23} corresponds to the movement of the proton from the uncoupler to the proton permeation pathway on the matrix side of AAC. The nature of this transition is unclear, as we do not know if it involves little-to-no protein motion, subtle conformational changes such as a rotamer flip, or a more substantial transition. That said, our analysis will show that this transition must occur very fast, comparable to ion movement rates between adjacent sites in potassium channel filters[74] and certain steps along the permeation pathway of the ClC-ec1 Cl^-/H^+ antiporter[75]. Thus, once AAC has undergone the transition to the proton conductive state, it is unlikely that the k_{23} transition rate corresponds to a large conformational change. Nonetheless, the ratio of the rates of

the proton moving from the uncoupler to the matrix pathway (k_{23} over k_{32}) is equal to the exponential of the energy difference between these states, as we discuss later.

Now assume that the rate of proton binding, in the absence of membrane potential, depends on the diffusion of bulk protons from the half-space above (cytoplasm/IMS) or below (matrix) the transporter to the respective protein entrance. We treat these two entrances as flat discs with radii r determined by the steric opening of the transporter to either space. The analytic solution to the diffusion equation for the rate of capture of protons to such a disk is follows (see Ref. [76]):

$$k_c^{on} = 0.6\, nm^{-3} \cdot 10^{-pH_c} \cdot 4r_c \cdot D_p \tag{4}$$

where r_c is the radius of the cytoplasmic facing opening based-on the AAC1 structure, D_p is the proton diffusion coefficient in nm^2/s, and 0.6 is a conversion factor so that Eq. (4) has the units of H^+/s. The first term ($0.6\, nm^{-3} \cdot 10^{-pH_c}$) represents the proton concentration, while the second ($4r_c \cdot D_p$) represents the adsorption rate at the entrance. This numeric pre-factor follows from dimensional analysis of the right- and left-hand sides of Eq. 4. Starting with the units of concentration, radius, and diffusion coefficient on the right-hand side, we have:

$$\left[\frac{moles}{(1000\ cm^3)} \cdot nm \cdot nm^2/s\right] = 6.02 \times 10^{23} \cdot 10^{-3} \cdot (10^{-7})^3 [\#/s] \approx 0.6\ [\#/s] \tag{5}$$

At equilibrium we have,

$$k_c^{on}[A^-] = k_c^{off}[AH] \tag{6}$$

where $[A^-]$ is the unprotonated small molecule uncoupler in the binding site, $[AH]$ is the protonated form, and k_c^{off} is the unbinding rate to the cytoplasm. The reverse rates can then be obtained from detailed balance using the definition of pK_a for the small molecules:

$$\frac{[A^-][H^+]_c}{[AH]} = 10^{-pK_a} = \frac{k_c^{off}[H^+]_c}{k_c^{on}} = \frac{k_c^{off}}{k_c^{on}} 10^{-pH_c} \tag{7}$$

$$\Rightarrow k_c^{off} = k_c^{on} \cdot 10^{-pK_a + pH_c} = 0.6 \cdot 4r_c \cdot D_p \cdot 10^{-pK_a} \tag{8}$$

where $[H^+]_c$ is the cytoplasmic proton concentration, and pK_a is the uncoupler's pK_a free in solution.

In the AAC1 binding pocket identified in the main text, the probability of finding the uncoupler protonated is biased by two primary factors: the total electrostatic energy E_{elec}, which includes contributions from the protein charges and the Born self-energy of the permeant ion, and the membrane electric field induced by membrane voltage V. We estimated both of these values by carrying out Poisson-Boltzmann electrostatics calculations on AAC1 as shown in Fig. 4f and Extended Data Fig. 10. Generally, we can write the electrostatic energy of a proton at the protonatable site of the molecule in AAC1 as:

$$\Delta E_{uncoupler} = E_{elec} + fVe \tag{9}$$

where E_{elec} is the total electrostatic energy of a proton-like molecule at the protonatable site in AAC1, f is the fraction of the membrane electrical the proton travels through from the cytoplasmic space to this site, and e is the fundamental charge unit. Since the conformation of the proton-conducting state is not known, we also do not know the value of f. Our best estimate for f is based on our c-state electrostatic calculations, which places f close to 0.1 (10% of the membrane electric field). However, If the conducting state involves opening of a rather wide, water filled cavity to the m-state with a concomitant narrowing of the cavity facing the c-state, then f would approach 0.5. Given this uncertainty, we explored f values ranging from 0.1 (blue curve) to 0.5 (green curve) in Extended Data Fig. 10c. We then modify the proton binding and unbinding rates using simple Eyring rate theory as follows:

$$k_c^{on} = (0.6 \cdot 4r_c \cdot D_p \cdot 10^{-pH_c}) \cdot exp\left(-\frac{1}{2} \cdot \frac{E_{elec}+fVe}{k_B T}\right) \tag{10}$$

$$k_c^{off} = (0.6 \cdot 4r_c \cdot D_p \cdot 10^{-pK_a}) \cdot exp\left(+\frac{1}{2} \cdot \frac{E_{elec}+fVe}{k_B T}\right) \tag{11}$$

where we assume that the impact of the electrostatic energy on the rates is equally split between the forward and reverse reactions, hence the factor of 1/2 in the exponents.

The energy of a proton in the matrix pathway (E_1) is not known, and we explore a range of values in Extended Data Fig. 10e accordingly from 0 to 10 $k_B T$. We write the rates of transfer between the uncoupler and pathway as a function of the energy difference:

$$\Delta E = E_1 - (E_{elec} + ln(10) \cdot pK_a) + gVe \tag{12}$$

where g is the fraction of the membrane electric field experienced by the proton moving from the uncoupler to the matrix pathway, which we assume is half the field from the uncoupler to the matrix: $1 = f + 2g$ or $g = (1 - f)/2$. Again applying an Eyring-like modification to the base rates, the corresponding rate constants are then:

$$k_{23} = a \cdot exp\left(-\frac{1}{2} \cdot \frac{\Delta E}{k_b T}\right) \quad (13)$$

$$k_{32} = a \cdot exp\left(+\frac{1}{2} \cdot \frac{\Delta E}{k_b T}\right) \quad (14)$$

and the sites automatically obey detailed balance. The prefactor a has units of inverse time. Sweeping through values of a with E_1 and other parameters fixed at the base values (Supplementary Table 2), it becomes clear that the H^+ current requires k_{23} to be in the upper nanosecond range or faster (Extended Data Fig. 10e) for efficient conduction or else the rate of the H^+ returning back to the cytoplasm dominates due to the large positive E_{elec} in the cavity. Moreover, I_H is insensitive to the energy of H^+ in the pathway (E_1) as long as the forward rate from the uncoupler to the pathway is fast, consistent with a number of proton permeation mechanisms (Extended Data Fig. 10e).

Next, the exchange of protons between the matrix pathway and the mitochondrial matrix can then be written as:

$$k_m^{on} = (0.6 \cdot 4r_m \cdot D_p \cdot 10^{-pH_m}) \cdot exp\left(-\frac{1}{2} \cdot \frac{E_1 - gVe}{k_B T}\right) \quad (15)$$

$$k_m^{off} = (0.6 \cdot 4r_m \cdot D_p) \cdot exp\left(+\frac{1}{2} \cdot \frac{E_1 - gVe}{k_B T}\right) \quad (16)$$

where the form of these equations follows that of Eqs. 10-11 for exchange with the cytoplasm/IMS and r_m is the radius of the pathway leading to the matrix.

The flux of protons from the cytoplasm/IMS into the transporter is J_1 and the flux into the matrix is J_2 defined by (negative flux indicates proton flux into the lumen):

$$J_1 = -(x_1 k_c^{on} - x_2 k_c^{off}) \quad \text{and} \quad J_2 = -(x_3 k_m^{off} - x_1 k_m^{on}) \quad (17)$$

At steady state, these two fluxes are equal, and they represent the overall proton current into or out of the mitochondria.

We calculated the ionic currents from this model (Eqs. 1-3) by numerically solving for the steady state solutions using the ODE15s solver in Matlab over a range of voltages (Fig. 4h), a range of uncoupler pK_a values (Extended Data Fig. 10d), and a range of uncoupler to matrix pathway transition rates k_{23} (Extended Data Fig. 10e) using the parameters in Supplementary Table 2.

Supplementary Text 2. Supplementary discussion

Our computational analysis of the AAC1 c-state supports the model that both FAs and chemical uncouplers exert their influence on the protein by binding within the translocation pathway. Intriguingly, the predicted binding sites for FAs and uncouplers appear to be different and located on the opposite sides of the AAC translocation pathway at the bottom of the cytosolic cavity. The simulations suggest that FAs are stabilized in AAC by two principal interactions: 1) the hydrophobic interaction of the aliphatic tail with the bilayer core and helices 5 and 6, and 2) electrostatic interactions between the negatively charged carboxylic headgroup and K22/R79/R279. However, because the interaction between the headgroup and K22/R79/R279 depends on the protonation state of the FA, the hydrophobic interaction is more crucial for retaining the FA within AAC during H^+ translocation. In contrast, hydrophobic interactions are not as important for the binding of chemical uncouplers because they also establish several specific polar and stacking interactions with AAC. FAs may also associate with the uncoupler binding site, but this association is transient unless another FA already occupies the principal FA binding site mentioned above.

Our mathematical model confirms the feasibility of uncoupler/FA-induced I_H through the central translocation pathway of AAC. That said, there are outstanding features that must be further probed experimentally, such the conformational change associated with uncoupler binding, which allows H^+ permeation. The predicted current under physiological pH gradients is 15 H^+/sec - significantly lower than those elicited by the voltage-gated H^+ channel Hv1 (10^4-10^5 H^+/sec)[77], but closely matching that estimated for UCP1[78] and viral H^+ channel M2[77]. Nonetheless, a robust amplitude of the whole-IMM I_H can still be achieved due to the very large membrane density of AAC. Despite the remaining questions raised by this analysis, the computational results presented here represent the first molecular-level model of FA- and uncoupler-induced I_H in AAC. Validation of this model will require future structure-function studies and development of an AAC heterologous expression system compatible with patch-clamp electrophysiology to enable the dissociation of the H^+ and nucleotide transport modes of AAC.

All chemical uncouplers examined in this work have two mechanisms of action, a protonophoric activity affecting all cell membranes and an IMM-specific H^+ leak via AAC and UCP1. Despite this, our data indicates that it might be possible to develop specific activators of mitochondrial I_H via AAC (UCP1) that lack the protonophoric activity. Indeed, a protonophore is a hydrophobic weak acid that can diffuse across the membrane both in the neutral and the negatively charged deprotonated forms to complete a H^+ translocation cycle. Charge delocalization from the protonatable group to the hydrophobic moiety is crucial for the membrane diffusion of the negatively charged form[10,11]. In contrast, an activator of I_H via AAC and UCP1 is a weak acid that interacts with an uncoupler binding site, using a combination of hydrophobic and polar interactions. Thus, some potential examples of I_H activators via AAC/UCP1without protonophoric activity would include those

with higher polarity and/or no charge delocalization between the protonatable and hydrophobic moieties to achieve low capacity for bilayer diffusion. Currently, long-chain FA, which lack charge delocalization, are the only example of AAC and UCP1 activators without protonophoric activity[7]. The low bioavailability makes long-chain FA unsuitable for pharmacological use, but our findings establish a framework for the development of novel specific activators of I_H via AAC and UCP1. Such next-generation anti-obesity and anti-diabetes drugs would activate native thermogenic pathways similar to their endogenous activators, long-chain FA, and might have improved safety in comparison with general protonophores.

References

74 Morais-Cabral, J. H., Zhou, Y. & MacKinnon, R. Energetic optimization of ion conduction rate by the K+ selectivity filter. *Nature* **414**, 37-42, doi:10.1038/35102000 (2001).

75 Mayes, H. B., Lee, S., White, A. D., Voth, G. A. & Swanson, J. M. J. Multiscale Kinetic Modeling Reveals an Ensemble of Cl(-)/H(+) Exchange Pathways in ClC-ec1 Antiporter. *J Am Chem Soc* **140**, 1793-1804, doi:10.1021/jacs.7b11463 (2018).

76 Crank, J. *The Mathematics of Diffusion*. (Oxford University Press, 1980).

77 Decoursey, T. E. Voltage-gated proton channels and other proton transfer pathways. *Physiol Rev* **83**, 475-579, doi:10.1152/physrev.00028.2002 (2003).

78 Urbankova, E., Voltchenko, A., Pohl, P., Jezek, P. & Pohl, E. E. Transport kinetics of uncoupling proteins. Analysis of UCP1 reconstituted in planar lipid bilayers. *J Biol Chem* **278**, 32497-32500, doi:10.1074/jbc.M303721200 (2003).